

# Influence of Reynolds Number on Flow and Heat Transfer Around Spherical and Non-Spherical Objects

E. SZYMANEK\* AND P. SZYMANEK

*Częstochowa University of Technology, 42-201 Częstochowa, Poland*

Doi: [10.12693/APhysPolA.139.606](https://doi.org/10.12693/APhysPolA.139.606)

\*e-mail: [ewaszym@imc.pcz.pl](mailto:ewaszym@imc.pcz.pl)

The article conducts an analysis of flow around spherical and non-spherical elements for a wide range of Reynolds numbers using direct numerical simulations based on the indefinite heat conducting equation (3D) and the Navier–Stokes equation. The research focuses on the influence of the shape of the element on the drag coefficient of the flow. It has been found that the total air drag coefficient around the considered elements depends on their shape and Reynolds number. The drag coefficient for the particular element example (sphere) has been compared with the experimental data. Further results have been presented in this paper.

topics: spherical and non-spherical element, heat transfer, drag coefficient, numerical modeling

## 1. Introduction

Over the years, many efforts have been made in order to examine the flow around spherical and non-spherical objects under different flow conditions. This is not only due to the need to better understand the parameters of such flows, but also because of their important practical implementations.

Most publications focus on spherical elements and the analyses of such flows are carried out within a wide range of Reynolds numbers. The situation is slightly different in the case of any other elements. Their shape and orientation in the stream significantly affect the flow. This fact is often not taken into account and that is why the number of references connected to the flow around non-spherical elements is considerably low. For example, Kumar [1] analyzed the flow around ellipsoids and spheres and Saha [2] conducted numerical research of liquid and heat exchange around a cube. Richter and Nikriyuk [3], in turn, focused on ellipsoidal rectangular particles in laminar flow systems, which are directed towards the stream.

It is worth pointing out that with exceptionally low Reynolds numbers, the movement around elements is dominated by resistance forces. The results show that changes to surface pressure and drag factors are a strong shape function.

The purpose of this paper is to provide data for a three-dimensional flow around ellipsoids of the circular and elliptical section as compared to the flow around a cube and sphere taking into account the drag coefficient.

## 2. Mathematical modeling

In this paper, we consider variable temperature and variable density flows. Changes of density are caused by the increasing/decreasing wall temperature and they are larger than acceptable by the Boussinesq approximation. We consider a low Mach number flow described by the continuity equation, the Navier–Stokes equations and the energy equation. In the framework of the Immersed Boundary Volume Penalization (IB–VP) approach, they are defined as:

$$\partial_t \rho + \nabla(\rho \mathbf{u}) = 0 \quad (1)$$

$$\rho \left( \partial_t \mathbf{u} + (\mathbf{u} \cdot \nabla) \mathbf{u} \right) + \nabla p = \nabla \cdot \boldsymbol{\tau} + f^{\text{IB}} \quad (2)$$

$$\rho C_p \left( \partial_t T + (\mathbf{u} \cdot \nabla) T \right) = \nabla \cdot (\kappa \nabla T) + f_T^{\text{IB}} \quad (3)$$

where  $\rho$  stands for the density,  $T$  — the temperature,  $p$  — the hydrodynamic pressure,  $\mathbf{u}$  — the velocity vector,  $C_p$  — the heat capacity and  $\kappa$  — the heat conductivity. The set of (1)–(3) is complemented with the equation of state  $p_0 = \rho R T$ , where  $p_0$  denotes the thermodynamic pressure and  $R$  is the specific gas constant. In open flows with inlet/outlet boundaries,  $p_0$  is constant in space and time and in this work it is assumed to be 101325 Pa. The molecular viscosity ( $\mu$ ) within the viscous stress tensor  $\boldsymbol{\tau}$  is computed from Sutherland's law.

The IB–VP method works through penalizing a difference between the actual and assumed velocity and temperature of the solid body. The role

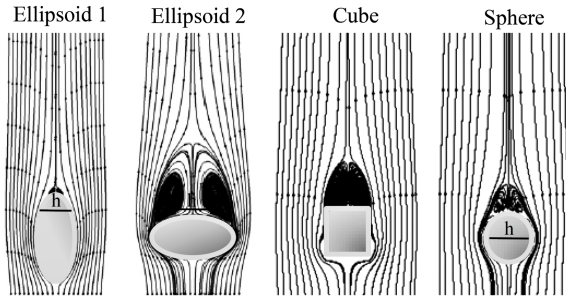


Fig. 1. Flow around various objects, streamlines for  $Re = 100$ .

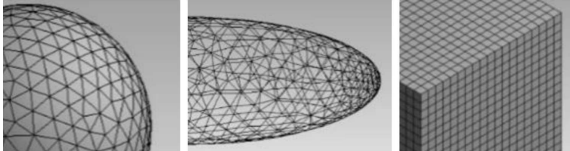


Fig. 2. Non-uniform computational grid structure.

of the source terms  $f^{IB}$  and  $f_T^{IB}$  is to mimic the presence of solid objects in the flow domain. In the volume penalization variant of the IB method they are defined as:

$$f^{IB} = -\frac{\rho}{\eta} \Gamma(x) (u - u_s), \quad (4)$$

$$f_T^{IB} = -\frac{\rho C_p}{\eta} \Gamma(x) (T - T_s), \quad (5)$$

where  $u_s$  and  $T_s$  are the velocity and temperature of the solid body, respectively.

The solution algorithm for (1)–(3) is formulated in the framework of a projection method [4] for pressure–velocity coupling. The time integration is based on a predictor–corrector approach (Adams–Bashforth/Adams–Moulton) and the spatial discretisation is performed using the 6th/5th order compact difference and WENO (Weighted Essentially NonOscillatory) schemes on half-staggered meshes [5, 6].

### 3. Computational domain

A rectangular computing domain with dimensions of  $L_x = 0.21$  m and  $L_z = L_y = 0.04$  m has been used in all cases. The flow was along the  $x$  axis. The uniform flow velocity in the inlet section is determined according to the Reynolds number. Simulations were carried out for Reynolds number  $Re = Uh/\nu = 100$  ( $U$  — inlet velocity,  $\nu$  — viscosity). The value of the  $h$  parameter was consequently selected as: shorter axis (ellipsoid 1), longer axis (ellipsoid 2), edge of the cube and the sphere's diameter. Figure 1 shows the considered element configurations and streamlines for the Reynolds number equal to 100.

It is assumed that the medium temperature at the intake was 300 K and the surface temperature of the element was constant and equalled 400 K. The simulations were conducted using the academic code

based on the IB–VP method on a regular grid consisting of  $128 \times 320 \times 128$  nodes and the commercial software Ansys Fluent adopted to the surface size computing grids consisting of about 1730000 cells (see Fig. 2).

### 4. Results

Sixteen different instances were simulated in order to examine the influence of the Reynolds number and the element shape on the drag coefficient. Figure 3 shows velocity and temperature distribution for all analysed elements with the Reynolds number equal to 100.

Referring to visible differences between the layouts, one can observe that the impact of the element shape is clear, and the biggest differences can be seen right behind the object. A more detailed analysis provides Figs. 4 and 5 where the velocity and temperature profiles along the flow are presented.

In order to verify the adopted method, the solutions obtained for the elements using Ansys code have been shown in Fig. 4 (points). The compliance of the solutions obtained with the IB–VP method

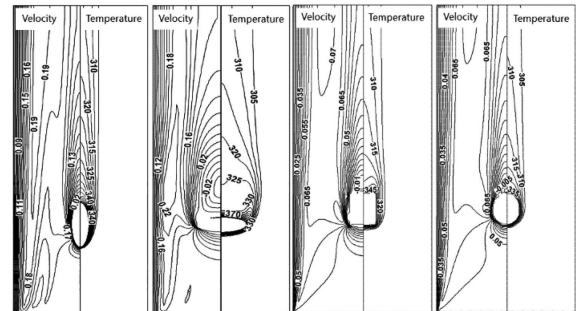


Fig. 3. Velocity [m/s] and temperature [K] contours,  $Re = 100$ .

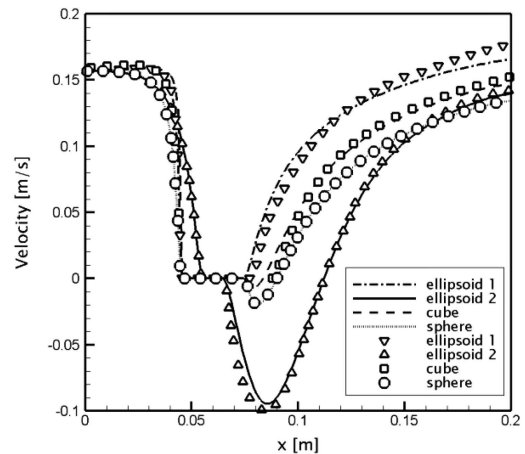


Fig. 4. Comparison of the results using the IB–VP method and the Ansys Fluent program (IB–VP results are marked with lines, Fluent results — with points) — velocity profiles along the flow,  $Re = 100$ .

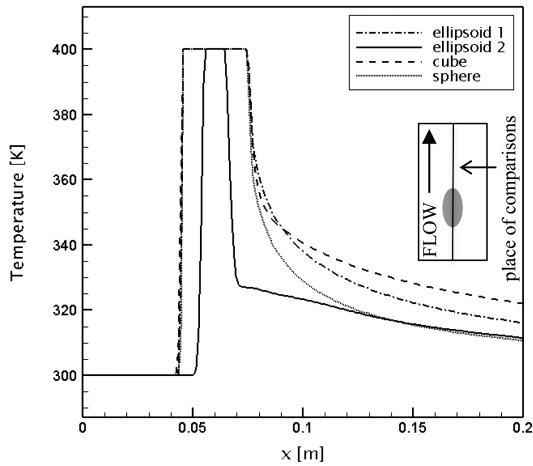


Fig. 5. Temperature profiles along the flow (using the IB-VP method),  $Re = 100$ .

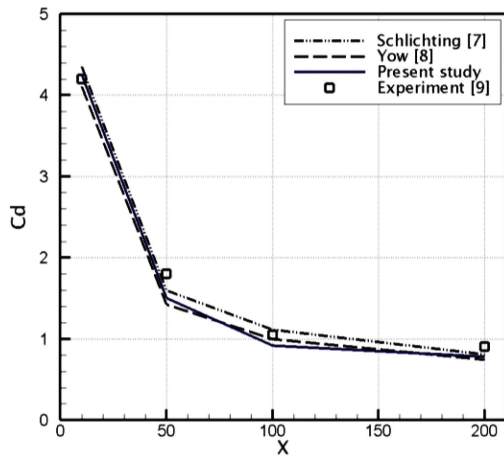


Fig. 6. Comparison of the numerical results (present study) with the literature data [7–9] for the sphere.

with Ansys Fluent code is very good. Even in areas right behind the element, the negative velocity values have been precisely calculated.

The presented profiles show results along the extracted line along the channel and going through the center of the elements. The highest velocity values have been noticed for ellipsoid 1. It is worth noticing that only behind this element the recirculation area was not present. The drop in the velocity value relates to different flow blocking. According to Fig. 5, similar temperature values were noted at the end of the channel for ellipsoid 2 and the sphere.

Figures 6 and 7 present comparable drag coefficient values at  $Re = 10, 50, 100, 200$  in empirical correlations suggested by Schlichting and Gersten [7], Yow et al. [8] and experimental data of Roos and Willmarth [9]. The graphs clearly show that the current outcomes are similar to the literature value. The differences in the obtained values result, among others, from the individually selected computing grids and the solution method.

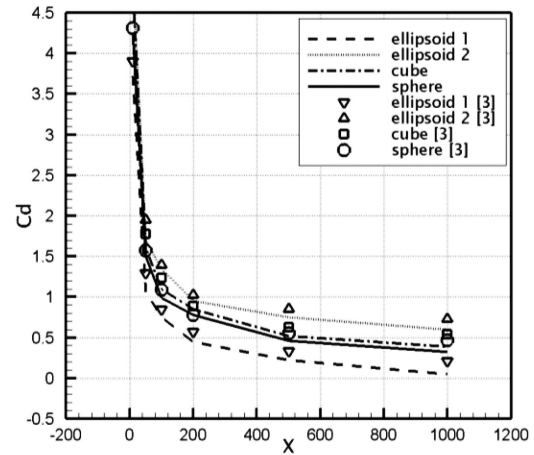


Fig. 7. Comparison of the results using the IB-VP method with literature data of Richter and Nikrityuk [3] (numerical results are marked with lines, literature data — with points).

It can be observed that regardless of the researched element, the total drag coefficients decrease with the increase of the Reynolds number. The obtained results reflect the variability of the drag coefficient well. Although we see differences between the literature values and the numerical ones (the highest have been noted for ellipsoids, especially for ellipsoid 1), they are very small. One can observe that the maximum error rate increases with the Reynolds number. Consequently, the maximum errors occur at  $Re = 1000$ . The highest deviation was observed for ellipsoid 1. Interestingly, only in the case of this element, a full symmetric flow field for the highest researched Reynolds number has been observed.

## 5. Conclusions

The purpose of this paper was to provide information about the flow around spherical and non-spherical elements. The presented research focused on the flow characteristics of heat and liquid around ellipsoids in two configurations, around a sphere and a cube. The first ellipsoid was positioned with its main axis along the flow, the second one was positioned perpendicularly. The calculations have been carried out with the Reynolds numbers equalling 10, 50, 100, 200, 500 and 1000 and using the academic code based on the IB-VP method. The outcomes have been verified by comparing them with the data obtained using the Ansys Fluent software. The comparisons of the numerical data have shown satisfactory compliance of all analysed cases. The numerical results presented in this paper show that the shape of the object affects the heat transfer rate. The drag coefficient has also been determined and compared with the literature data. Regardless of the shape of the element, the drag coefficient decreases with increasing Reynolds number. More

sufficient changes in the values of the drag coefficient were recorded for smaller Reynolds numbers. It has been determined that the influence of the shape on the drag coefficient is more significant for small Reynolds number values.

#### Acknowledgments

This work was supported by statutory funds of the Czestochowa University of Technology BS/PB-1-100-3016/2021/P and the National Science Centre, Poland (Grant No. 2017/27/N/ST8/02318). PL-Grid infrastructure was used to carry out the computations.

#### References

- [1] N. Kumar, S. Duvvuri, *Int. J. Pure Appl. Math.* **120**, 7929 (2018).
- [2] A.K. Saha, *Int. J. Heat Fluid Flow* **27**, 80 (2006).
- [3] A. Richter, P.A. Nikrityuk, *Powder Technol.* **249**, 463 (2013).
- [4] C.A.J. Fletcher, *Computational Techniques for Fluid Dynamics*, Springer-Verlag, Berlin 1991.
- [5] A. Tyliczszak, *Comp. Fluids* **127**, 131 (2016).
- [6] A. Tyliczszak, E. Szymanek, *Numer. Heat Transf. A* **76**, 737 (2019).
- [7] H. Schlichting, K. Gersten, *Boundary-Layer Theory*, Springer, Berlin 2003.
- [8] H.N. Yow, M.J. Pitt, A.D. Salman, *Adv. Powder Technol.* **16**, 363 (2005).
- [9] F.W. Roos, W.W. Willmarth, *AIAA J.* **9**, 285 (1971).